

"Glass-quake" in elastically loaded bulk metallic glasses

Qi Huang(黄琦), Kaiguo Chen(陈开果), Chen Liu(刘辰), Guisen Liu(刘桂森), Yang Shao(邵洋), Chenlong Zhao(赵晨龙), Ran Chen(陈然), Hengtong Bu(卜亨通), Lingti Kong(孔令体), and Yao Shen(沈耀)

Citation: Chin. Phys. B, 2024, 33 (**11**): 116402. DOI: 10.1088/1674-1056/ad7725
Journal homepage: http://cpb.iphy.ac.cn; http://iopscience.iop.org/cpb

What follows is a list of articles you may be interested in

Effect of Y element on atomic structure, glass forming ability, and magnetic properties of FeBC alloy

Jin-Hua Xiao(肖晋桦), Da-Wei Ding(丁大伟), Lin Li(李琳), Yi-Tao Sun(孙奕韬), Mao-Zhi Li(李茂枝), and Wei-Hua Wang(汪卫华)

Chin. Phys. B, 2024, 33 (**7**): 076101. DOI: 10.1088/1674-1056/ad3dd4

Structural origin for composition-dependent nearest atomic distance in Cu-Zr metallic glass

Chi Zhang(张驰), Hua-Shan Liu(刘华山), and Hai-Long Peng(彭海龙)

Chin. Phys. B, 2023, 32 (**11**): 116101. DOI: 10.1088/1674-1056/acce99

Migration of weakly bonded oxygen atoms in a-IGZO thin films and the positive shift of threshold voltage in TFTs

Chen Wang(王琛), Wenmo Lu(路文墨), Fengnan Li(李奉南), Qiaomei Luo(罗巧梅), and Fei Ma(马飞)†

Chin. Phys. B, 2022, 31 (**9**): 096101. DOI: 10.1088/1674-1056/ac560f

Crystallization evolution and relaxation behavior of high entropy bulk metallic glasses using microalloying process

Danhong Li(李丹虹), Changyong Jiang(江昌勇), Hui Li(栗慧), and Mahander Pandey

Chin. Phys. B, 2021, 30 (**6**): 066401. DOI: 10.1088/1674-1056/abd92c

Decline of nucleation in the heating process with a high heating rate

Yang Gao-Lin (杨高林), Lin Xin (林鑫), Song Meng-Hua (宋梦华), Hu Qiao (胡桥), Wang Zhi-Tai (汪志太), Huang Wei-Dong (黄卫东)

Chin. Phys. B, 2014, 23 (**8**): 086401. DOI: 10.1088/1674-1056/23/8/086401

"Glass-quake" in elastically loaded bulk metallic glasses

Qi Huang(黄琦)[1], Kaiguo Chen(陈开果)[2,†], Chen Liu(刘辰)[3,‡], Guisen Liu(刘桂森)[1,§], Yang Shao(邵洋)[4], Chenlong Zhao(赵晨龙)[1], Ran Chen(陈然)[1], Hengtong Bu(卜亨通)[4], Lingti Kong(孔令体)[1,5], and Yao Shen(沈耀)[1,¶]

[1] *State Key Laboratory of Metal Matrix Composites, School of Materials Science and Engineering, Shanghai Jiao Tong University, Shanghai* 200240, *China*
[2] *College of Science, National University of Defense Technology, Changsha* 410073, *China*
[3] *Independent Researcher, Paris, France*
[4] *School of Materials Science and Engineering, Tsinghua University, Beijing* 100084, *China*
[5] *Materials Genome Initiative Center, Shanghai Jiao Tong University, Shanghai* 200240, *China*

(Received 25 April 2024; revised manuscript received 11 July 2024; accepted manuscript online 4 September 2024)

Amorphous solids exhibit scale-free avalanches, even under small external loading, and thus can work as suitable systems to study critical behavior and universality classes. The abundance of scale-free avalanches in the entire elastic tension regime of bulk metallic glass (BMG) samples has been experimentally observed using acoustic emission (AE) measurements. In this work, we compare the statistics of avalanches with those of earthquakes, and find that they both follow the Gutenberg–Richter law in the statistics of energies and Omori's law of aftershock rates, and share the same characteristics in the distribution of recurrence times. These resemblances encourage us to propose the term "glass-quake" to describe avalanches in elastically loaded BMGs. Furthermore, our work echoes the potential universality of critical behavior in disordered physical systems from atomic to planetary scales, and motivates the use of elastic loaded BMGs as valuable laboratory simulators of seismic dynamics.

Keywords: bulk metallic glass, avalanche, earthquake, disorder system, time series

PACS: 64.60.av, 61.43.Dq, 91.30.Px, 61.43.–j **DOI:** 10.1088/1674-1056/ad7725

1. Introduction

Amorphous solids, including bulk metallic glasses (BMGs), colloids, and granular materials, play an important role in industries because of their unique properties.[1–4] Unlike crystalline solids, amorphous materials exhibit liquid-like characteristics stemming from two fundamental features of their states: structure disorder[5–8] and out of equilibrium state.[3,8,9] It is crucial to understand the fundamental physics underlying the elasticity of amorphous systems because of its importance in non-equilibrium statistical physics.

Recently, we experimentally observed abundant avalanches in elastically deformed metallic glass for the first time and investigated their statistical features and possible underlying fundamental physics.[10] Avalanches in elastically deformed amorphous solids were found to follow power-law statistics. This indicates that the amorphous deformation activities are correlated in space and time, naturally classifying this behavior as a form of critical phenomena. Inspired by the universality classes in critical phenomena, some studies have established the similarity between the avalanche dynamics in material, or structural compression, and in earthquakes, including the compression of single crystals,[11,12] rocks,[11,13,14] granular materials[11,15–17] and porous materials.[11,18,19]

Several empirical laws have been established for the statistical features of earthquakes. The Gutenberg–Richter law[20] states that the probability density distribution of earthquake energy follows a power law, i.e., $p(E) \propto E^{-\tau}$ (with $\tau = 1 + 2b$ and b close to 1). Clustering has been observed for the events when studying the time intervals (waiting times) between consecutive seismic events.[21,22] The power law features of the events inside the clusters indicate temporal correlations among intra-cluster events. Conversely, the presence of a gamma distribution is observed[23] when analyzing the statistics of waiting times between clusters. This suggests that distinct clusters are uncorrelated, and could be categorized as a Poisson-like process. Additionally, Omori's law[24] states that the rate of aftershocks, $N(t_{\rm as})$, after a main shock decays approximately inversely with the elapsed time $t_{\rm as}$, i.e., $N(t_{\rm as}) \propto t_{\rm as}^{-1}$.

In this paper, we report the presence of the Gutenberg–Richter law, the cluster features of recurrence times and Omori's law for avalanches in elastically loaded bulk metallic glasses. By combining the results of the above analysis, remarkably, we found that the avalanches witnessed during the tensile elastic deformation of BMG samples exhibit striking similarities to earthquake statistics, which strengthen the no-

†Corresponding author. E-mail: chenkaiguo@nudt.edu.cn
‡Corresponding author. E-mail: chen.liu.428@hotmail.com
§Corresponding author. E-mail: liuguisen@sjtu.edu.cn
¶Corresponding author. E-mail: yaoshen@sjtu.edu.cn

© 2024 Chinese Physical Society and IOP Publishing Ltd

tion of universality among disordered systems. These findings encourage us to propose the term "glass-quake" to describe avalanches in elastically loaded BMGs, and boost the idea that the avalanches observed during the elastic tension of metallic glass could serve as a convenient and controllable laboratory model for studying seismic events, in addition to previous compression models.[11–19]

2. Results

In our experiment, specimens of BMG ($Zr_{51}Cu_{28}Ni_9Al_{12}$) are subjected to axial tensile stress at a strain rate $\dot{\varepsilon} = 5 \times 10^{-4}$ s^{-1} at room temperature (far below the glass transition temperature $T_g = 705$ K), while the AE signals originating from avalanche events generated within BMG are recorded. For each BMG sample, $\sim 10^5$ avalanche events can be detected throughout the elastic deformation process. A single avalanche event is manifested as a time series of voltage signals, beginning with a voltage jump above the mean background of the AE waveform. A conventional threshold-based hit detection algorithm was applied to the recorded AE waveform $V(t)$ to identify AE events.[25] After the AE event identification, the AE waveform is converted to an AE events series $\{E_i\}$, with each event E_i characterizing an avalanche event. For each avalanche event, the energy of event S_i is defined as the area below the squared voltage curve as

$$S_i = \int_{t_{b,i}}^{t_{e,i}} V^2(t)\,\mathrm{d}t, \tag{1}$$

where $t_{b,i}$ and $t_{e,i}$ denote the start and end time of the ith event. To catch the evolution of avalanche dynamics during the course of the tensile test, statistical analysis is performed in each consecutively sliced 30 s time window, centered at a certain instant t, which can be equivalently translated to a total deformation $\varepsilon = \dot{\varepsilon}t$.

The waiting time $t_{w,i}$ of the ith avalanche is defined as the time interval between the end of this avalanche and the beginning of the next,

$$t_{w,i} = t_{b,i+1} - t_{e,i}. \tag{2}$$

Using the above methods, we obtained the avalanche energy series $\{S_i\}$ and the waiting time series $\{t_{w,i}\}$ from the raw signals received by the acoustic emission detector. For more details of the experiments, detection and statistics of avalanches, refer to the supplementary material.

2.1. Energy distribution of avalanches

The avalanche energy distribution in the entire elastic regime follows the Gutenberg–Richter law given by $P(S) \propto S^{-\tau}$, as illustrated in Fig. 1(a), validated for events occurring within time windows centered at four different levels of strain (or stress). Although a rigorous estimating procedure[26] suggests that the exponent τ decreases mildly from approximately 1.73 at the onset of deformation to around 1.48 at the failure (inset of Fig. 1), it is also legitimate to assert a non-varying mean-field value $\tau \approx 1.5$ for the entire range of deformation, as illustrated by the fair alignment between the distributions and the reference line in Fig. 1. The analysis of the avalanche energy distribution, as demonstrated in Fig. 1, reveals a power-law pattern similar to the renowned GR law.

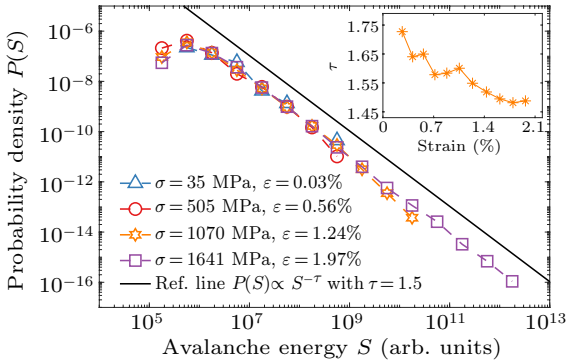


Fig. 1. Power-law distribution $P(S) \propto S^{-\tau}$ of avalanche energies S at different stress/strains. The inset shows the evolution of the exponent τ with strain.

In the statistical analysis of earthquakes, the size distribution of earthquakes is considered to follow a power-law distribution. This power-law distribution in earthquakes is also commonly referred to as the Gutenberg–Richter law (GR law) in seismology, which indicates the scale-free feature of earthquakes. GR law can be expressed using the following formula:

$$\log N = a - bM, \tag{3}$$

where N is the cumulative number of events above magnitude M.[20]

In GR law, the exponent b (or $\tau = 1 + 2b$) is an important parameter that quantifies the scale-free statistical behavior. A significant decrease in the b value prior to the occurrence of large earthquakes has been observed in numerous seismic activities. Basically, the b value can serve as an important indicator for predicting catastrophic earthquakes.[27–30] Furthermore, there is a linear negative correlation between the b value and differential stress (difference between the maximum and the minimum principal stress), with a smaller b value corresponding to greater differential stress, which is also a significant cause of major disasters.[31,32]

Like the conclusions drawn from b value research, as the deformation proceeds, the exponent τ of the avalanche power-law statistics in BMG samples also decreases with the increase in stress levels, as shown in Fig. 1. Consequently, it is inferred that an energy accumulation process that is comparable to that preceding a significant earthquake occurs during the elastic deformation of BMGs. This also suggests the presence of a potential underlying physical mechanism that connects the yielding transition in BMGs with catastrophic major earthquakes.

2.2. Fractal features of time series

The temporal clustering property of avalanches is analyzed by investigating the distribution of events over time and the distribution of waiting times between events. A clustering property can be clearly identified by naked eyes for the time series of events when zoomed into an appropriate time scale, as shown in the upper section of Fig. 2(a), where each dot represents an avalanche event with an attached vertical line indicating its time coordinate. Events separated by relatively small intervals gather into clusters and different clusters are separated by relatively large time intervals. To investigate the clustering properties, we first plot the probability distribution $Q_\varepsilon(t_w)$ of all the inter-avalanche waiting times t_w sampled within each time window centered at four different stress/strain levels, as shown in Fig. 2(b). At the early stage of the elastic regime, $Q_\varepsilon(t_w)$ displays a clear bimodal distribution with two populations that are respectively concentrated around a small value of $t_w \approx 10^{-4}$ s and a larger value $t_w \approx 10^{-0}$ s. As the deformation proceeds (as the stress increases), the two populations reach out towards each other and eventually join at a waiting time $t_w \approx 600$ μs (inset of Fig. 2(b)) when the stress reaches about half of the elastic limit. We go ahead to systematically group a series of events into clusters by inserting cluster boundaries whenever a pair of neighboring events are separated by a waiting time larger than t_w^*. Clusters produced in this way are vividly revealed using alternating red and blue colors in Fig. 2(a) (lower section), rendering t_w^* a quantitative criterion to classify the events into clusters.

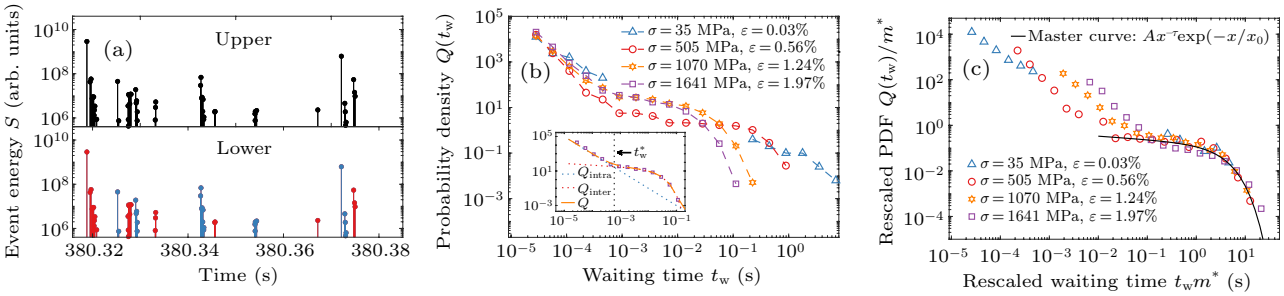


Fig. 2. Clustering features of an avalanche sequence. (a) Upper section: events represented by dots. Lower section: clustering of events based on the characteristic waiting time $t_w^* \approx 600$ μs, with consecutive clusters represented by alternating blue and red colors. (b) The waiting time distribution at different stress/strains. The inset shows the fitting of the purple group ($\sigma = 1641$ MPa) using the forms: $Q_{intra} = At_w^{-2}Q_{inter} = Bt_w^{-0.3}\exp(-t_w/0.015)$, and $Q = Q_{intra} + Q_{inter}$. The characteristic waiting time t_w^*, and the dividing intra- and inter-cluster waiting time distribution is determined by the intersection of Q_{intra} and Q_{inter}. (c) The waiting time distribution rescaled by the corresponding avalanche rate m^* at different stress/strains. The rescaled Q_{inter} parts collapse into a master curve, $A(t_w m^*)^{-0.15}\exp((-t_w m^*)/2.5)$.

Further analysis of $Q_\varepsilon(t_w)$ enables the distinction between intra- and inter-cluster behavior, indicating significantly different underlying physics between dynamics within and between clusters. With t_w^* severing as the separation point, the waiting time distribution within clusters follows a power-law distribution characterized by $Q_{intra}(t_w) \propto (t_w)^{-a}$, while the waiting time distribution between clusters follows a gamma distribution described by $Q_{inter}(t_w) \propto (t_w)^{-\phi}\exp(-t_w/t_{w_0})$. At a stress level of 1641 MPa, our data shows a $a \approx 2$ for the intra-cluster component and $\phi \approx 0.3$ for the inter-cluster component, which are obtained by fitting $Q_\varepsilon(t_w)$ using an additive model $\hat{Q}(t_w) = Q_{intra}(t_w) + Q_{inter}(t_w)$, as visually depicted in the inset of Fig. 2(b). These statistical features suggest that avalanche events within a cluster arise from strong spatial–temporal cooperative processes, displaying scaling invariant fractal features indicated by the power-law distribution of waiting times. In contrast, different clusters represent a separated and less cooperative processes, as the gamma distribution is typically associated with extreme events in independent processes. Additionally, the inter-cluster distribution Q_{inter} aligns with the predictions of the pseudo-gap theory in that the measured value of ϕ falls within a range that is consistent with numerical results on the pseudo-gap distribution in the elastic regime.[33,34] Thus, our inter-cluster waiting time may be considered as the thermal-finite-rate extension of the pseudo-gap that separates two successive avalanches in the athermal quasi-static driving condition. On one hand, the superposition of Q_{intra} for all the time windows in Fig. 2(b) unveils a universal and robust intra-cluster dynamics that remains unchanged under different strain/stress conditions. On the other hand, the universal pattern of inter-cluster dynamics is elucidated by a master curve that is obtained by rescaling the waiting time distribution $Q(t_w)$ with the measured avalanche rate m^* for each time window (Fig. 2(c)), which suggests an intrinsically invariant mode of random occurrence of cluster.

The statistics and the physical implications for the intra- and inter-cluster behavior share remarkable similarities to those of earthquakes. The re-scaled waiting time distributions depicted in Fig. 2(c) exhibit similarities to the recurrence time statistics of earthquakes.[23,35] Both the avalanche sequence and earthquake series display master curves that resemble gamma functions and possess comparable characteristic parameters. This suggests a shared temporal behavior between avalanches and earthquakes, characterized by an unknown dynamic mechanism that is common to both phenomena.

In statistical analysis of the waiting time series following avalanches with large or small waiting times, it is observed

that the conditional probability distributions of these two categories are not the same, with longer waiting times often followed by longer waiting times, and shorter waiting times followed by shorter waiting times. This phenomenon of clustering of long and short waiting times is considered as the memory effect in the temporal sequence.[36]

To investigate the memory effect, we first sort all avalanche waiting times and select those with the longest waiting times, which constitute a quarter of the total count (categorized as the 'longest quarter'). Subsequently, we calculate the probability density function for the waiting times of avalanches occurring subsequently to these long-waiting-time avalanches. Similarly, we perform the same operation for avalanches with shorter waiting times, also representing a quarter of the total (categorized as the 'shortest quarter'). Finally, we obtain two conditional probability density distributions, as shown in Figs. 3(a) and 3(b). The probability distributions of the waiting time of BMG avalanches, conditioned on a long or short prior waiting time value, exhibit similarity at low stress levels but become distinctly different at higher stress levels (Figs. 3(a) and 3(b)). This statistical feature indicates the emergence of a memory effect, which is a common finding in earthquake series,[36] during the elastic deformation of BMG.

Finally, the distribution of the aftershock rate as a function of the time distance to the main shock resembles Omori's law observed in earthquake statistics (Fig. 3(c)), up to a limit of a mean inter-cluster waiting time t_{w}^{*}. This lends support to the notion that similar dynamics may be shared by aftershocks of earthquakes and intra-cluster events of elastically deformed BMGs.

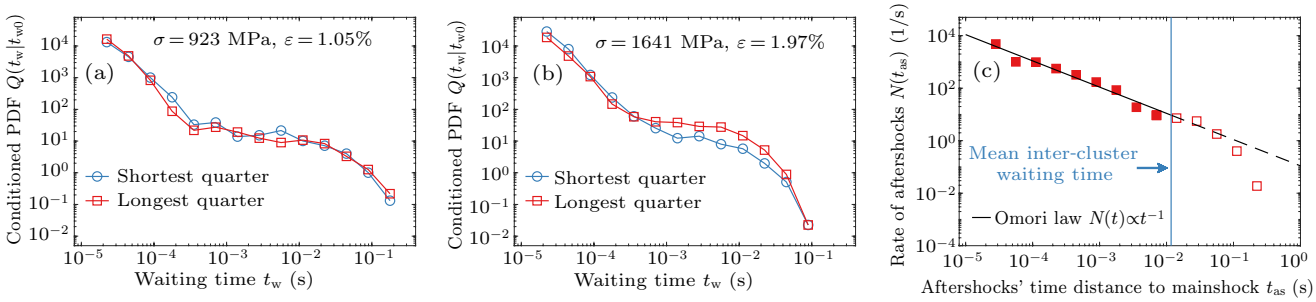


Fig. 3. Analogy to earthquake characteristics. (a) Conditioned probability distributions of the waiting time t_{w} following a waiting time t_{w0} either from the shortest quarter of all sorted waiting times (shortest quarter, circles) or the longest quarter of all sorted waiting times (longest quarter, squares) of all t_{w0}s at a medium stress level of 923 MPa. (b) Conditioned probability distributions similar to (a) but at a higher stress level of 1641 MPa. (c) The rate of aftershocks N as a function of the time distance of the aftershocks t_{as} to the main shock. The main shock is defined as the energy of AE events exceeding 2.29×10^{7}. Solid and open squares represent t_{as} values below and above the mean intra-cluster waiting time, respectively.

3. Concluding remarks: Glass-quake

These wide and strong similarities to earthquakes suggest the utilization of BMG as a convenient laboratory simulator for the investigation of earthquake dynamics. BMG distinguishes itself from other seismic simulators[16,19,37,38] in that the size ratio between the entire system and the elementary excitation can be readily achieved up to $\sim 10^{7}$, which is comparable with that of earthquakes, while other laboratory simulators usually achieve a size ratio that is 1000–10000 times smaller. Such a full range representation is desirable for faithfully revealing the underlying scale-free dynamics proportionally down scaled from the earthquakes.

Our results on the statistical behavior of avalanche events in glasses reveal striking similarities to earthquakes, leading us to coin the term "glass-quake" to describe this phenomenon. The emergence of the glass-quake suggests a potential universality in the "interplay of disorder and fluctuations in physical systems from the atomic to the planetary scales".[38] Beyond the vivid potential for experimental data generation through the use of BMGs as a convenient simulator, the field of glass physics may offer valuable insights into advancing our understanding of earthquake dynamics. In particular, concepts such as the complex potential energy landscape, pseudo gap, and marginal stability, which are commonly employed to describe the dynamics of amorphous systems, may serve as a novel avenue for laboratory-scale investigations of earthquakes. The continued development of experimental and theoretical techniques will help to further our understanding of the relationship between glass-quake and earthquake dynamics, and ultimately lead to new insights into the underlying physics of these complex systems.

Acknowledgements

Project supported by the National Natural Science Foundation of China (Grant Nos. 51801122 and 52071210), the Science Challenge Project (Grant No. TZ2018001), and the Science and Technology Commission of Shanghai (Grant No. 21ZR1430800).

References

[1] Berthier L, Biroli G, Bouchaud J P, Cipelletti L and van Saarloos W 2011 *Dynamical heterogeneities in glasses, colloids, and granular media* Vol. 150 (OUP Oxford)
[2] Inoue A, Kong F, Zhu S and Greer A 2019 *MRS Bulletin* **44** 867
[3] Berthier L and Biroli G 2011 *Rev. Mod. Phys.* **83** 587

[4] Sun Y, Concustell A and Greer A L 2016 *Nature Reviews Materials* **1** 16039
[5] Finney J 1970 *Proc. Roy. Soc. London. A Math. Phys. Sci.* **319** 479
[6] Sheng H, Luo W, Alamgir F, Bai J and Ma E 2006 *Nature* **439** 419
[7] Yang Y, Zhou J, Zhu F, *et al.* 2021 *Nature* **592** 60
[8] Charbonneau P, Kurchan J, Parisi G, Urbani P and Zamponi F 2017 *Annual Review of Condensed Matter Physics* **8** 265
[9] Bonn D, Denn M M, Berthier L, Divoux T and Manneville S 2017 *Rev. Mod. Phys.* **89** 035005
[10] Huang Q, Chen K, liu C, Liu G, Shao Y, Zhao C, Chen R, Bu H, Kong L and Shen Y, to be published
[11] Uhl J T, Pathak S, Schorlemmer D, Liu X, Swindeman R, Brinkman B A W, LeBlanc M, Tsekenis G, Friedman N, Behringer R, Denisov D, Schall P, Gu X, Wright W J, Hufnagel T, Jennings A, Greer J R, Liaw P K, Becker T, Dresen G and Dahmen K A 2015 *Scientific Reports* **5** 16493
[12] Ispánovity P D, Ugi D, Péterffy G, Knapek M, Kalácska S, Tüzes D, Dankházi Z, Máthis K, Chmelík F and Groma I 2022 *Nat. Commun.* **13** 1975
[13] Lockner D 1993 *International Journal of Rock Mechanics and Mining Sciences & Geomechanics Abstracts* **30** 883
[14] Salje E K H, Lampronti G I, Soto-Parra D E, Baró J, Planes A and Vives E 2013 *American Mineralogist* **98** 609
[15] Ferdowsi B, Griffa M, Guyer R A, Johnson P A, Marone C and Carmeliet J 2015 *Geophysical Research Letters* **42** 9750
[16] Lherminier S, Planet R, Vehel V L dit, Simon G, Vanel L, Måløy K J and Ramos O 2019 *Phys. Rev. Lett.* **122** 218501
[17] Johnson P A, Savage H, Knuth M, Gomberg J and Marone C 2008 *Nature* **451** 57
[18] Nataf G F, Castillo-Villa P O, Baró J, Illa X, Vives E, Planes A and Salje E K H 2014 *Phys. Rev. E* **90** 022405
[19] Baró J, Corral Á, Illa X, Planes A, Salje E K H, Schranz W, Soto-Parra D E and Vives E 2013 *Phys. Rev. Lett.* **110** 088702
[20] Gutenberg B and Richter C F 1944 *Bulletin of the Seismological Society of America* **34** 185
[21] Bak P, Christensen K, Danon L and Scanlon T 2002 *Phys. Rev. Lett.* **88** 178501
[22] Karsai M, Kaski K, Barabási A L and Kertész J 2012 *Scientific Reports* **2** 397
[23] Corral 2004 *Phys. Rev. Lett.* **92** 108501
[24] Utsu T, Ogata Y and Matsu'ura S R 1995 *Journal of Physics of the Earth* **43** 1
[25] Unnpórsson R 2013 *Hit detection and determination in AE bursts Acoustic emission-research and applications* 1–20
[26] Clauset A, Shalizi C R and Newman M E J 2009 *SIAM Review* **51** 661
[27] Nanjo K Z, Hirata N, Obara K and Kasahara K 2012 *Geophysical Research Letters* **39** L20304
[28] Mousavi S M, Ogwari P O, Horton S P and Langston C A 2017 *Physics of the Earth and Planetary Interiors* **267** 53
[29] Xie W, Hattori K, Han P and Shi H 2022 *Entropy* **24** 494
[30] Gulia L and Wiemer S 2019 *Nature* **574** 193
[31] Schorlemmer D, Wiemer S and Wyss M 2005 *Nature* **437** 539
[32] Scholz C H 2015 *Geophysical Research Letters* **42** 1399
[33] Xu H, Andresen J C and Regev I 2021 *Phys. Rev. E* **103** 052604
[34] Hentschel H G E, Jaiswal P K, Procaccia I and Sastry S 2015 *Phys. Rev. E* **92** 062302
[35] Zaliapin I and Ben-Zion Y 2016 *Geophysical Journal International* **207** 608
[36] Livina V N, Havlin S and Bunde A 2005 *Phys. Rev. Lett.* **95** 208501
[37] Stojanova M, Santucci S, Vanel L and Ramos O 2014 *Phys. Rev. Lett.* **112** 115502
[38] Barés J, Dubois A, Hattali L, Dalmas D and Bonamy D 2018 *Nat. Commun.* **9** 1253
[39] Parisi G 2023 Nobel Lecture: *Multiple equilibria*